J Bras Pneumol. 2021;47(2):e20200055
https://dx.doi.org/10.36416/1806-3756/e20200055

ORIGINAL ARTICLE

MRI-based differentiation between lymphoma and sarcoidosis in mediastinal lymph nodes

Francisco de Souza Santos[1], Nupur Verma[2], Edson Marchiori[3], Guilherme Watte[1], Tássia M Medeiros[1], Tan-Lucien H Mohammed[2], Bruno Hochhegger[1]

1. Programa de Pós-Graduação em Medicina e Ciências da Saúde, Faculdade de Medicina, Pontifícia Universidade Católica do Rio Grande do Sul, Porto Alegre (RS) Brasil.
2. Department of Radiology, University of Florida, Gainesville (FL) USA.
3. Departamento de Radiologia, Universidade Federal do Rio de Janeiro, Rio de Janeiro (RJ) Brasil.

Submitted: 11 February 2020.
Accepted: 29 November 2020.

Study carried out at the Instituto do Cérebro – InsCer – Porto Alegre (RS) Brasil.

ABSTRACT

Objective: Evaluation of enlarged mediastinal lymph nodes is crucial for patient management. Malignant lymphoma and sarcoidosis are often difficult to differentiate. Our objective was to determine the diagnostic accuracy of MRI for differentiating between sarcoidosis and malignant lymphoma. **Methods:** This was a retrospective study involving 47 patients who underwent chest MRI and were diagnosed with one of the diseases between 2017 and 2019. T1, T2, and diffusion-weighted signal intensity were measured. Apparent diffusion coefficients (ADCs) and T2 ratios were calculated. The diagnostic performance of MRI was determined by ROC analysis. **Results:** Mean T2 ratio was significantly lower in the sarcoidosis group than in the lymphoma group (p = 0.009). The T2-ratio cutoff value that best differentiated between lymphoma-related and sarcoidosis-related enlarged lymph nodes was 7.1, with a sensitivity, specificity, positive predictive value, negative predictive value, and accuracy of 58.3%, 95.6%, 76.5%, 93.3%, and 68.7%, respectively. The mean ADC was significantly lower in the lymphoma group than in the sarcoidosis group (p = 0.002). The ADC cutoff value that best differentiated between lymphoma-related and sarcoidosis-related enlarged lymph nodes was 1.205, with a sensitivity, specificity, positive predictive value, negative predictive value and accuracy of 87.5%, 82.6%, 85.1%, 84.0% and 86.3%, respectively. No significant differences were found between the two groups regarding T1 signal intensity, T2 signal intensity, and lymph node diameter. **Conclusions:** MRI parameters such as ADC, diffusion, and T2 ratio can be useful in the differentiation between sarcoidosis and lymphoma in the evaluation of enlarged lymph nodes.

Keywords: Diffusion magnetic resonance imaging; Lymphoma; Lymph nodes; Sarcoidosis.

INTRODUCTION

The evaluation of mediastinal lymph nodes is clinically essential for effective disease management and accurate prognosis.[1] Various infectious, inflammatory, and malignant conditions can cause mediastinal lymph node enlargement. Sarcoidosis is a benign systemic disorder of unknown etiology that frequently underlies thoracic diseases, chest abnormalities being seen in 85-95% of the patients who undergo chest X-ray.[2] In contrast, lymphoma is a malignant tumor of the lymphatic system that arises in lymphocytes. Interestingly, not only do these two conditions affect the lymph nodes, but the age at onset of both also overlaps. As such, the adenopathy caused by lymphoma can be confused with sarcoidosis upon initial detection even after imaging.[3]

When mediastinal lymph node enlargement occurs, histopathological analysis is the recommended means of obtaining a definitive diagnosis, providing a prognosis and determining which treatment course is best suited to manage the disease. However, interventional access to the mediastinum entails inherent risks for patients and sampling error. It also places a psychological burden on the patient during the period between the detection of the adenopathy by imaging methods and sampling results. Imaging techniques are very efficient in locating and evaluating enlarged mediastinal nodes.[4-6]

A readily available, primary technique for evaluating thoracic diseases is CT imaging. Despite being a well-established technique for pulmonary evaluation when used to assess lymph nodes, CT relies on morphological characteristics such as location, size, and distribution of lymph nodes. Cases of sarcoidosis with atypical findings and uncertain diagnosis can mimic other pathologies; the appearance of lymph nodes on CT scans can even resemble malignant disease.[7,8] Thus, the use of CT imaging is limited when it comes to distinguishing between

Correspondence to:
Francisco de Souza Santos. Instituto do Cérebro – InsCer – Avenida Ipiranga, 6690, CEP 90610-000, Porto Alegre, RS, Brasil.
Tel.: 55 51 98411-7187. Fax: 55 51 3320-3454. E-mail: franciscodesouzasantos@gmail.com
Financial support: Francisco de Souza Santos and Tássia Machado Medeiros received financial support from the Brazilian *Coordenação de Aperfeiçoamento de Pessoal de Nível Superior* (CAPES, Office for the Advancement of Higher Education; Funding Code 001). Edson Marchiori and Bruno Hochhegger received financial support from the Brazilian *Conselho Nacional de Desenvolvimento Científico e Tecnológico* (CNPq, National Council for Scientific and Technological Development).

malignant and benign enlarged lymph nodes.[7,9-12] PET-CT, a metabolic imaging technique, has promising yet controversial diagnostic potential for differentiation between granulomatous and malignant disease.[13,14] Although PET-CT is helpful for detecting malignant disease, it is more expensive, less accessible, and lacks specificity when compared with traditional CT.[15,16] In this scenario, MRI is a radiation-free, highly reproducible technique that is well-suited for lymph node assessment.[17] The lack of ionizing radiation makes it particularly appealing for evaluating young adults with symptoms that merely resemble malignancy. MRI sequences, such as diffusion-weighted imaging (DWI), can also provide quantitative metrics that facilitate effective lymph node characterization.[18-24]

The purpose of the present study was to determine the diagnostic accuracy of MRI for differentiating between sarcoidosis and lymphoma by quantitative evaluation of mediastinal lymph nodes in patients with either condition.

METHODS

Our institutional review board approved this study. Patient consent was waived due to the retrospective nature of the study. The authors have no conflicts of interest to declare.

Study population

This retrospective study included 47 consecutive adult patients from our institution who underwent chest MRI and were histopathologically diagnosed with either sarcoidosis or lymphoma over the course of two years (between January of 2017 and January of 2019). The diagnosis of sarcoidosis was based on the three major criteria recommended by the American Thoracic Society[25]: compatible clinical presentation, exclusion of alternative causes of granulomatous nodules, and histopathological evidence of non-necrotizing granulomatous inflammation. Patients whose MRI assessment was performed after treatment initiation were excluded from the analysis. Patients with recent thoracic interventions, radiation therapy initiated prior to MRI acquisition, or an active concomitant infectious disease were also excluded. Clinical data were obtained from the electronic medical records of the patients (Tasy EMR, Philips Clinical Informatics, Blumenau, Brazil).

MRI protocol

MRI was performed using a 1.5-T scanner (Magnetom AERA; Siemens Healthineers, Erlangen, Germany). A dedicated 8-element integrated matrix coil system covering the entire thorax was used for signal reception. A half-Fourier acquisition single-shot turbo spin-echo sequence was used. The following sequence parameters were used: repetition time (TR)/echo time (TE)/flip angle, infinite/92 ms/150°; parallel acquisition factor, 2; slice thickness, 5 mm; distance factor, 20%; and matrix size, 380 × 256 mm (transversally) and 400 × 320 mm (coronally). A volumetric interpolated breath-hold examination (VIBE) sequence was chosen for fast T1-weighted MRI. For the VIBE sequence, imaging parameters were as follows: TR/TE, 5.12 ms/2.51 ms; flip angle, 10°; partition thickness, 5 mm with no interslice gap; and matrix size, 256 × 116 mm, with a three-dimensional breath-hold imaging technique. A T2-weighted fat-saturated periodically rotated overlapping parallel lines with enhanced reconstruction sequence (BLADE; Siemens Healthineers) was also used, imaging parameters being as follows: TR/TE, 4,670 ms/113 ms; and partition thickness, 5 mm with no interslice gap. DWI was performed using a single-shot echo-planar technique, with a slice thickness of 6 mm under spectral attenuated inversion recovery and respiratory-triggered scanning. DWI parameters were as follows: TR/TE/flip angle, 3,000-4,500 ms/65 ms/90°; diffusion gradient encoding in three orthogonal directions; b = 0 and 800 s/mm^2; field of view, 350 mm; and matrix size, 128 × 128 mm. Imaging parameters are summarized in Table 1.

Image analysis

The MRI files were independently reviewed by two subspecialized chest radiologists who were blinded to patient clinical information and final diagnoses. When differences of opinion arose between the radiologists, a consensus was reached.

The largest lymph node from each patient was visually selected by the radiologist on the T2-weighted image. An elliptical two-dimensional region of interest was drawn around the chosen lymph node area on T2-weighted, T1-weighted, DWI, and apparent diffusion coefficient (ADC) map reconstructions. Necrotic regions were avoided. An elliptical region of interest was also placed around the adjacent latissimus dorsi muscle for T2-ratio determination. The T2 ratio was calculated by the signal intensity of the lymph node ($S_{T2\ lymph\ node}$) divided by the signal intensity of the latissimus dorsi muscle ($S_{T2\ skeletal\ muscle}$) on a T2-weighted image (i.e., T2 ratio = $S_{T2\ lymph\ node}/S_{T2\ skeletal\ muscle}$). Lymph node location, dimensions, and signal intensity (T1, T2, and diffusion-weighted signal intensity), as well as ADC, were recorded.

Statistical analysis

The data are presented as frequency and proportion, mean ± SD, or median [IQR]. The relationships between categorical variables were assessed using chi-square tests. To compare continuous variables, the Student's t-test or the unequal variance t-test was used. Sensitivity, specificity, positive predictive value, and negative predictive value of the MRI findings were calculated in relation to the corresponding histopathological diagnosis. Kappa coefficients were calculated to determine the inter-rater agreement using a 2 × 2 contingency table. A 95% CI was used. In all cases, the level of statistical significance was set at $p < 0.05$. All statistical analyses were performed using the IBM SPSS Statistics software package, version 22.0 (IBM Corporation, Armonk, NY, USA).

RESULTS

A total of 51 consecutive patients were initially included in the study. Three patients were excluded because they initiated treatment prior to undergoing MRI. One patient with a previous diagnosis of sarcoidosis was excluded because he eventually had a definitive diagnosis of tuberculosis. The remaining 47 patients with histopathology-based diagnoses of sarcoidosis or lymphoma were included in the study. A flow chart of the patient selection process is depicted in Figure 1. In our sample, 27 patients (57%) were men. The mean age of the patients was 51 ± 17 years. All of the patients were biopsied via mediastinoscopy. Of the 47 included patients, 23 (47%) had sarcoidosis and 24 (53%) had lymphoma. In the lymphoma group, 20 patients had non-Hodgkin's B-cell lymphoma and 4 had nodular sclerosing Hodgkin's lymphoma.

The mean diameters (including both short and long axis diameters) were 1.62 ± 0.60 cm in the sarcoidosis group and 2.78 ± 0.83 cm in the lymphoma group. In the sarcoidosis group, the largest lymph nodes were located in the subcarinal (n = 19) and right paratracheal (n = 4) spaces. In the lymphoma group, the largest lymph nodes were found in the subcarinal (n = 20), right hilar (n = 2), left paratracheal (n = 1), and left hilar (n = 1) spaces. Of the 23 patients with sarcoidosis, 20 had typical parenchymal CT findings of interstitial micronodules.[26] One patient exhibited pulmonary fibrosis, and 2 patients presented with no signs of pulmonary disease.

Table 1. Imaging parameters of the MRI protocol of the study.

Parameter	T1-weighted VIBE	T2-weighted fat-saturated PROPELLER	HASTE		DWI
Orientation	Transverse	Transverse	Transverse	Coronal	Transverse
TR (ms)/TE (ms)/FA (°)	5.12/2.51/10	4,670/113	infinite/92/150	infinite/92/150	3,000-4,500/65/90
FOV (mm)	Patient adapted	Patient adapted	Patient adapted	Patient adapted	350
Matrix (mm)	256 × 116	256 × 256	380 × 256	400 × 320	128 × 128
Slice thickness (mm)	5	5	5	5	6
Gating	No	Respiratory	No	No	Respiratory
Breath holding	Yes	No	Yes	Yes	No

VIBE: volumetric interpolated breath-hold examination (sequence); PROPELLER: periodically rotated overlapping parallel lines with enhanced reconstruction (sequence); HASTE: half-Fourier acquisition single-shot turbo spin-echo (sequence); DWI: diffusion-weighted imaging; TR: repetition time; TE: echo time; FA: flip angle; and FOV: field of view.

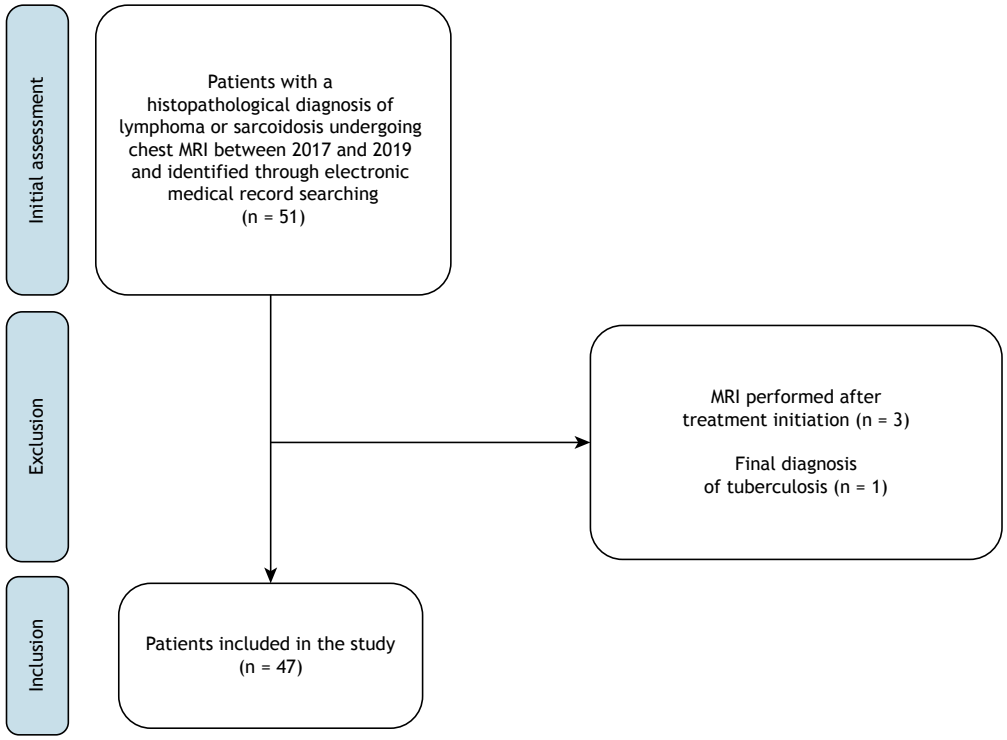

Figure 1. Flow chart of the patient selection process.

There were no significant differences between the two groups in terms of T1 signal intensity, T2 signal intensity, lymph node location, or lymph node size. The mean T2 ratio was significantly lower in the sarcoidosis group than in the lymphoma group (5.0 [3.7-5.3] and 8.3 [4.9-11.9], respectively; p = 0.009), as was the mean diffusion of the lymph nodes (22 [19-54] and 58 [24-96], respectively; p = 0.003). The mean ADC was significantly lower in the lymphoma group than in the sarcoidosis group (0.993 ± 0.508 × 10^{-3} mm^2/s vs. 1.668 ± 0.732 × 10^{-3} mm^2/s; p = 0.002). A ROC curve indicated that an ADC cutoff value of 1.205 × 10^{-3} mm^2/s was optimal for differentiating between lymph nodes affected by lymphoma and those affected by sarcoidosis. Using this cutoff value, sensitivity, specificity, positive predictive value, negative predictive value, and accuracy were 87.5%, 82.6%, 85.1%, 84.0%, and 86.3%, respectively. The T2 ratio cutoff value that best differentiated between lymphoma-affected and sarcoidosis-affected lymph nodes was 7.1, with a sensitivity, specificity, positive predictive value, negative predictive value, and accuracy of 58.3%, 95.6%, 76.5%, 93.3%, and 68.7%, respectively. A kappa coefficient of 0.69 reflected substantial inter-rater agreement. A comprehensive comparison of the MRI findings between the sarcoidosis and lymphoma groups is shown in Table 2. Figures 2 and 3 exemplify our findings.

DISCUSSION

Given that pulmonary sarcoidosis can mimic several other pathologies, including malignant causes of adenopathy,[8] the differentiation between sarcoidosis and such pathologies is crucial for ensuring optimal patient outcomes. The importance of precise imaging-based diagnoses has motivated extensive research on more specific and sensitive means of determining the causes underlying lymph node enlargement. Mehrian & Ebrahimzadeh[12] used CT scans in order to identify variations in the site and morphology of thoracic lymph nodes that correlated differentially with sarcoidosis and lymphoma. Koo et al.[14] demonstrated that there was no significant difference between lymph nodes affected by sarcoidosis or malignant lymphoma using PET-CT, reinforcing the similarity between these pathologies and the difficulty of reaching a definitive diagnosis even with advanced imaging techniques. In the present study, MRI evaluation illuminated characteristics of enlarged mediastinal lymph nodes that have reliably and reproducibly distinguished between sarcoidosis and lymphoma.

Previous studies have also used MRI to differentiate between malignant and benign lymph node pathologies successfully using DWI- and ADC-based quantitative measurements.[18-24] Diffusion evinces the mobility of water molecules within tissues. Cellularity is a common pathological feature that is characteristic of neoplasms, restricting the movement of water molecules and thereby reducing their diffusion. However, lymph node enlargement caused by benign diseases (e.g., infection, congestive heart failure, and drug-induced lymphadenopathy) is more likely to increase diffusion. Due to the aforementioned characteristic of cellularity, MRI is not effective in differentiating subtypes of neoplasms. For example, Matoba et al.[27] found that the ADC values of lymph nodes affected by metastatic small cell carcinomas were not significantly different than those of lymph nodes affected by non-small cell carcinomas. Our results confirmed that ADC values of lymph nodes affected by malignant lymphoma were significantly lower than those of lymph nodes affected by sarcoidosis. Diffusion measurements also differed significantly, with lower values in the sarcoidosis group than in the malignant lymphoma group. The findings of the present study support the use of DWI and ADC mapping as an effective and accurate resource for distinguishing between mediastinal lymph nodes affected by either malignant or benign diseases.

Only patients who underwent MRI prior to initiating treatment were included in the present study, because the impact of treatment on DWI findings remains undetermined. Lymph node size and cellularity could change upon therapeutic intervention, as could tumor size and ADC values. One study[28] used DWI to evaluate lymph node eradication after chemoradiation therapy in patients with locally advanced rectal cancer, but no additional diagnostic benefit was conferred by adding DWI to the T2 imaging findings. In contrast, another study[29] found that DWI is more accurate

Table 2. Comparison of parameters between patients diagnosed with either sarcoidosis (n = 23) or lymphoma (n = 24).[a]

Parameter	Sarcoidosis	Lymphoma	p
Male	12 (52)	15 (62)	0.561
Age, years	49 ± 14	53 ± 18	0.406
Short axis diameter, cm	1.54 ± 0.48	1.69 ± 0.69	0.940
Long axis diameter, cm	2.73 ± 1.00	2.83 ± 0.65	0.474
T1	215 ± 96	159 ± 73	0.031
T2	190 [156-260]	126 [96-222]	0.123
DWI	22 [19-54]	58 [24-96]	0.003
ADC, × 10^{-3} mm^2/s	1.668 ± 0.732	0.993 ± 0.508	0.002
T2 ratio	5.0 [3.7-5.3]	8.3 [4.9-11.9]	0.009

DWI: diffusion-weighted imaging; and ADC: apparent diffusion coefficient. [a]Values expressed as n (%), mean ± SD, or median [IQR].

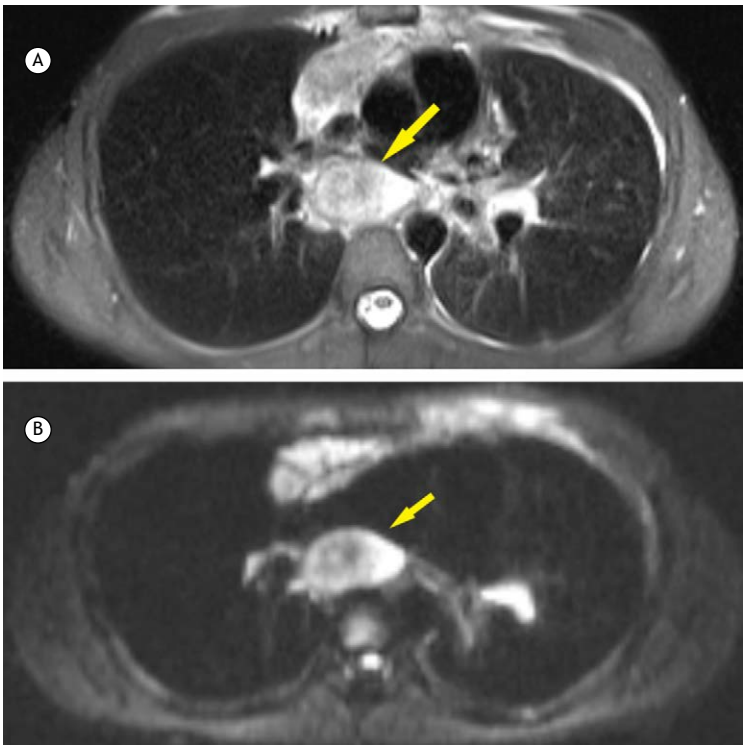

Figure 2. Transverse MRI scans of a 35-year-old man with sarcoidosis. In A, T2-weighted PROPELLER MRI of an enlarged mediastinal lymph node. In B, apparent diffusion coefficient (ADC) map reconstruction of the lymph node. PROPELLER: periodically rotated overlapping parallel lines with enhanced reconstruction. ADC = 1.74 × 10^{-3} mm^2/s.

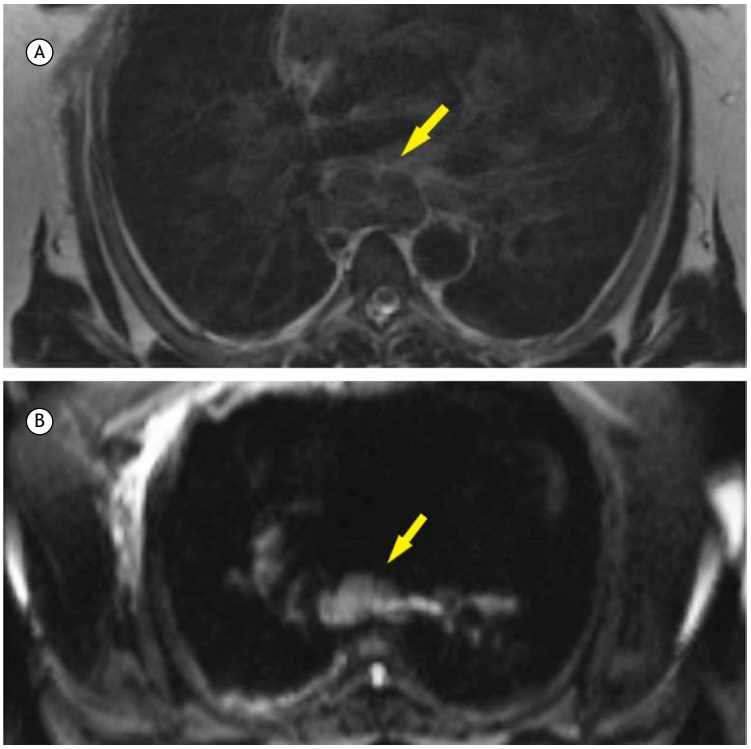

Figure 3. Transverse MRI scans of a 17-year-old man with Hodgkin lymphoma. In A, T2-weighted PROPELLER MRI of an enlarged mediastinal lymph node. In B, apparent diffusion coefficient (ADC) map reconstruction of the lymph node. PROPELLER: periodically rotated overlapping parallel lines with enhanced reconstruction. ADC = 0.9 × 10^{-3} mm^2/s.

than CT when assessing response to radiation therapy, chemotherapy, or both.

An important finding from this study is that the T2 ratio is lower in sarcoidosis-affected lymph nodes than in lymphoma-affected lymph nodes. The use of T2 ratio in our study is justified to avoid interindividual differences, such as those frequently caused by receiver-coil bias. The correlation between fibrotic and calcified contents in sarcoidosis-related lymph node enlargement is likely to be the cause of the lower T2 ratio found in our study, which aligns with the aforementioned literature. The T2 ratio was more specific but less accurate than ADC values in differentiating between mediastinal lymph nodes enlarged due to either lymphoma or sarcoidosis.

Chung et al.[30] described the dark lymph node sign, an MRI finding that is characteristic of lymph nodes affected by sarcoidosis. A possible correlation with fibrotic content may underlie the dark lymph node sign—a node with low internal intensity and hyperintensity along the peripheral rim on T2-weighted imaging. That study,[30] however, did not include patients with malignant diseases, such as lymphoma, which restricts their findings to granulomatous diseases. Moreover, they did not measure the signal intensity and based their findings on a largely qualitative evaluation of the imaging examination.

Our study has some limitations. The retrospective nature of the study carries inherent selection biases, and the data obtained from the electronic medical records of the patients could potentially be inaccurate, which could affect our results. Another limitation was the small number of patients with atypical findings of sarcoidosis on MRI imaging. Although no patients had active tuberculosis infection, the subjects were recruited from a population highly affected by the disease. Any selection bias in our research criteria could have prevented the inclusion of patients during the study period if the terms lymph nodes, sarcoidosis, or lymphoma were not cited in the medical reports. Although we controlled the MRI evaluation performed by the radiologists by using quantitative measurement parameters, another limitation is the inter-rater variability regarding the selection of the largest lymph node, lymph node measurements, and MRI signal quantification. Future studies should include cases of patients with enlarged mediastinal lymph nodes caused by other conditions (e.g., metastases, infectious diseases, and other inflammatory conditions). Quantitative evaluation of enlarged lymph nodes due to diseases other than sarcoidosis and lymphoma represents an important addition to the understanding of the behavior of lymphadenopathies within the context of different thoracic diseases.

In conclusion, MRI-based indications of diffusion and T2 ratio can facilitate the differentiation between sarcoidosis-related and lymphoma-related enlarged mediastinal lymph nodes. Although the T2 ratio was more specific but less accurate than ADC values, their combined ability to make such a crucial clinical distinction using MRI data represents an invaluable diagnostic advancement that is particularly relevant for young patients presenting with sarcoidosis or lymphoma, whose symptoms are highly similar.

AUTHOR CONTRIBUTIONS

FSS and BH: study conception and design, literature search, and acquisition and interpretation of data; GW: statistical analyses; FSS, GW, TMM, and THM: drafting of the manuscript; BH, EM, NV, THM, and TMM: critical revision of the manuscript for important intellectual content; BH: supervision, data integrity, and guarantor of the article.

REFERENCES

1. Pannu HK, Wang KP, Borman TL, Bluemke DA. MR imaging of mediastinal lymph nodes: evaluation using a superparamagnetic contrast agent. J Magn Reson Imaging. 2000;12(6):899-904. https://doi.org/10.1002/1522-2586(200012)12:6<899::AID-JMRI13>3.0.CO;2-R
2. Lynch JP 3rd, Ma YL, Koss MN, White ES. Pulmonary sarcoidosis. Semin Respir Crit Care Med. 2007;28(1):53-74. https://doi.org/10.1055/s-2007-970333
3. Frampas E. Lymphomas: Basic points that radiologists should know. Diagn Interv Imaging. 2013;94(2):131-144. https://doi.org/10.1016/j.diii.2012.11.006
4. Major Complications of Videomediastinoscopy and their Resolution - a 5 year experience. Rev Port Cir Cardiotorac Vasc. 2017;24(3-4):138.
5. Gupta S, Seaberg K, Wallace MJ, Madoff DC, Morello FA Jr, Ahrar K, et al. Imaging-guided percutaneous biopsy of mediastinal lesions: different approaches and anatomic considerations. Radiographics. 2005;25(3):763-788. https://doi.org/10.1148/rg.253045030
6. Goldberg SN, Raptopoulos V, Boiselle PM, Edinburgh KJ, Ernst A. Mediastinal lymphadenopathy: diagnostic yield of transbronchial mediastinal lymph node biopsy with CT fluoroscopic guidance-initial experience. Radiology. 2000;216(3):764-767. https://doi.org/10.1148/radiology.216.3.r00se32764
7. Ganeshan D, Menias CO, Lubner MG, Pickhardt PJ, Sandrasegaran K, Bhalla S. Sarcoidosis from Head to Toe: What the Radiologist Needs to Know. Radiographics. 2018;38(4):1180-1200. https://doi.org/10.1148/rg.2018170157
8. Hawtin KE, Roddie ME, Mauri FA, Copley SJ. Pulmonary sarcoidosis: the 'Great Pretender'. Clin Radiol. 2010;65(8):642-650. https://doi.org/10.1016/j.crad.2010.03.004
9. Prenzel KL, Mönig SP, Sinning JM, Baldus SE, Brochhagen HG, Schneider PM, et al. Lymph node size and metastatic infiltration in non-small cell lung cancer. Chest. 2003;123(2):463-467. https://doi.org/10.1378/chest.123.2.463
10. Seely JM, Mayo JR, Miller RR, Müller NL. T1 lung cancer: prevalence of mediastinal nodal metastases and diagnostic accuracy of CT. Radiology. 1993;186(1):129-132. https://doi.org/10.1148/radiology.186.1.8416552
11. Wu Y, Li P, Zhang H, Shi Y, Wu H, Zhang J, et al. Diagnostic value of fluorine 18 fluorodeoxyglucose positron emission tomography/computed tomography for the detection of metastases in non-small-cell lung cancer patients. Int J Cancer. 2013;132(2):E37-E47. https://doi.org/10.1002/ijc.27779
12. Mehrian P, Ebrahimzadeh SA. Differentiation between sarcoidosis and Hodgkin's lymphoma based on mediastinal lymph node involvement pattern: Evaluation using spiral CT scan. Pol J Radiol. 2013;78(3):15-20. https://doi.org/10.12659/PJR.889056
13. Steinert HC, Hauser M, Allemann F, Engel H, Berthold T, von Schulthess GK, et al. Non-small cell lung cancer: nodal staging with FDG PET versus CT with correlative lymph node mapping and sampling. Radiology. 1997;202(2):441-446. https://doi.org/10.1148/

radiology.202.2.9015071

14. Koo HJ, Kim MY, Shin SY, Shin S, Kim SS, Lee SW, et al. Evaluation of Mediastinal Lymph Nodes in Sarcoidosis, Sarcoid Reaction, and Malignant Lymph Nodes Using CT and FDG-PET/CT. Medicine (Baltimore). 2015;94(27):e1095. https://doi.org/10.1097/MD.0000000000001095
15. Roberts PF, Follette DM, von Haag D, Park JA, Valk PE, Pounds TR, et al. Factors associated with false-positive staging of lung cancer by positron emission tomography. Ann Thorac Surg. 2000;70(4):1154-1160. https://doi.org/10.1016/S0003-4975(00)01769-0
16. Nomori H, Mori T, Ikeda K, Kawanaka K, Shiraishi S, Katahira K, et al. Diffusion-weighted magnetic resonance imaging can be used in place of positron emission tomography for N staging of non-small cell lung cancer with fewer false-positive results. J Thorac Cardiovasc Surg. 2008;135(4):816-822. https://doi.org/10.1016/j.jtcvs.2007.10.035
17. Guimaraes MD, Schuch A, Hochhegger B, Gross JL, Chojniak R, Marchiori E. Functional magnetic resonance imaging in oncology: state of the art. Radiol Bras. 2014;47(2):101-111. https://doi.org/10.1590/S0100-39842014000200013
18. Nakayama J, Miyasaka K, Omatsu T, Onodera Y, Terae S, Matsuno Y, et al. Metastases in mediastinal and hilar lymph nodes in patients with non-small cell lung cancer: quantitative assessment with diffusion-weighted magnetic resonance imaging and apparent diffusion coefficient. J Comput Assist Tomogr. 2010;34(1):1-8. https://doi.org/10.1097/RCT.0b013e3181a9cc07
19. Abdel Razek AA, Gaballa G, Elashry R, Elkhamary S. Diffusion-weighted MR imaging of mediastinal lymphadenopathy in children. Jpn J Radiol. 2015;33(8):449-454. https://doi.org/10.1007/s11604-015-0434-1
20. Sigovan M, Akl P, Mesmann C, Tronc F, Si-Mohamed S, Douek P, et al. Benign and malignant enlarged chest nodes staging by diffusion-weighted MRI: an alternative to mediastinoscopy?. Br J Radiol. 2018;91(1082):20160919. https://doi.org/10.1259/bjr.20160919
21. Usuda K, Maeda S, Motono N, Ueno M, Tanaka M, Machida Y, et al. Diagnostic Performance of Diffusion-Weighted Imaging for Multiple Hilar and Mediastinal Lymph Nodes with FDG Accumulation. Asian Pac J Cancer Prev. 2015;16(15):6401-6406. https://doi.org/10.7314/APJCP.2015.16.15.6401
22. Qi LP, Yan WP, Chen KN, Zhong Z, Li XT, Cai K, et al. Discrimination of Malignant versus Benign Mediastinal Lymph Nodes Using Diffusion MRI with an IVIM Model. Eur Radiol. 2018;28(3):1301-1309. https://doi.org/10.1007/s00330-017-5049-8
23. Abdel Razek AA, Elkammary S, Elmorsy AS, Elshafey M, Elhadedy T. Characterization of mediastinal lymphadenopathy with diffusion-weighted imaging. Magn Reson Imaging. 2011;29(2):167-172. https://doi.org/10.1016/j.mri.2010.08.002
24. Koşucu P, Tekinbaş C, Erol M, Sari A, Kavgaci H, Oztuna F, et al. Mediastinal lymph nodes: assessment with diffusion-weighted MR imaging. J Magn Reson Imaging. 2009;30(2):292-297. https://doi.org/10.1002/jmri.21850
25. Crouser ED, Maier LA, Wilson KC, Bonham CA, Morgenthau AS, Patterson KC, et al. Diagnosis and Detection of Sarcoidosis. An Official American Thoracic Society Clinical Practice Guideline. Am J Respir Crit Care Med. 2020;201(8):e26-e51. https://doi.org/10.1164/rccm.202002-0251ST
26. Criado E, Sánchez M, Ramírez J, Arguis P, de Caralt TM, Perea RJ, et al. Pulmonary sarcoidosis: typical and atypical manifestations at high-resolution CT with pathologic correlation. Radiographics. 2010;30(6):1567-1586. https://doi.org/10.1148/rg.306105512
27. Matoba M, Tonami H, Kondou T, Yokota H, Higashi K, Toga H, et al. Lung carcinoma: diffusion-weighted mr imaging–preliminary evaluation with apparent diffusion coefficient. Radiology. 2007;243(2):570-577. https://doi.org/10.1148/radiol.2432060131
28. Ryu KH, Kim SH, Yoon JH, Lee Y, Paik JH, Lim YJ, et al. Diffusion-weighted imaging for evaluating lymph node eradication after neoadjuvant chemoradiation therapy in locally advanced rectal cancer. Acta Radiol. 2016;57(2):133-141. https://doi.org/10.1177/0284185114568908
29. Usuda K, Iwai S, Funasaki A, Sekimura A, Motono N, Matoba M, et al. Diffusion-weighted magnetic resonance imaging is useful for the response evaluation of chemotherapy and/or radiotherapy to recurrent lesions of lung cancer. Transl Oncol. 2019;12(5):699-704. https://doi.org/10.1016/j.tranon.2019.02.005
30. Chung JH, Cox CW, Forssen AV, Biederer J, Puderbach M, Lynch DA. The dark lymph node sign on magnetic resonance imaging: a novel finding in patients with sarcoidosis. J Thorac Imaging. 2014;29(2):125-129. https://doi.org/10.1097/RTI.0b013e3182a4378b